Cyclotron-Stark-phonon-photon resonances in semiconductor superlattices under terahertz irradiation

1999 J. Phys.: Condens. Matter 11 2539

(http://iopscience.iop.org/0953-8984/11/12/009)

J. Phys.: Condens. Matter **11** (1999) 2539–2549. Printed in the UK PII: S0953-8984(99)00014-4

Cyclotron–Stark–phonon–photon resonances in semiconductor superlattices under terahertz irradiation

P Kleinert† and V V Bryksin‡

† Paul-Drude-Institut für Festkörperelektronik, Hausvogteiplatz 5-7, 10117 Berlin, Germany
‡ Physical Technical Institute, Politekhnicheskaya 26, 194021 St Petersburg, Russia

Received 8 December 1998

Abstract. High-field transport of electrons in semiconductor superlattices under intense parallel magnetic and time-dependent electric fields is investigated within a quantum-kinetic approach. Intra-collisional field effects of all fields are taken into account. In a biased superlattice subject to an intense radiation field of terahertz frequency, cyclotron–Stark–phonon–photon current resonances are predicted to occur for particular ratios of the Bloch (Ω_{dc}), cyclotron (ω_c), and terahertz frequencies (ω). Under strong irradiation, pronounced maxima appear at resonance positions given by $l\Omega_{dc} + n\omega_c + m\omega \pm \omega_0 = 0$, where l, n, m are integers and ω_0 the phonon frequency. Electro-phonon resonances are enhanced by a magnetic field but strongly weakened by an intense terahertz electric field.

1. Introduction

A strong electric field applied parallel to the superlattice (SL) axis localizes electronic states along the field direction into Wannier–Stark (WS) states, whose spatial extent is inversely proportional to the field strength. If the level broadening $\hbar/\tau_{dc}$ is smaller than the spacing $eE_{dc}d$ (where E_{dc} is the dc electric field and d the SL period) between the rungs of the WS ladder, the current proceeds by inelastic hopping between WS states belonging to neighbouring SL wells. The increase of the degree of localization with the electric field gives rise to negative differential conductance (NDC) in the current–voltage (I–V) characteristic. It has been predicted [1–3] that WS quantization leads to electro-phonon resonances at $leE_{dc}d = \hbar\omega_0$ (where ω_0 is the frequency of polar-optical phonons and l an integer) giving rise to a non-monotonic I–V dependence. Such resonances are greatly enhanced by a parallel magnetic field [4], which quantizes the lateral electron motion. If both fields are applied, the energy spectrum becomes completely discrete. Related cyclotron–Stark–phonon resonances have been studied both experimentally [5–10] and theoretically [4, 11–13].

An ac field in the terahertz (THz) domain, also applied parallel to the SL axis, opens up a second transport channel due to delocalization of carriers in the irradiation field accompanied by resonant photon absorption. The radiation field can suppress the formation of field domains and can thus contribute to a stabilization of the I–V characteristics in the NDC regime. Under the condition that Bloch oscillations interfere resonantly with the THz field ($\Omega_{dc} = k\omega$, where $\Omega_{dc} = eE_{dc}d/\hbar$ is the Bloch frequency, k any integer, and ω the frequency of the THz field), carrier motion against the field direction becomes resonant by absorbing the energy of photons [14]. This may lead to an absolute negative current as has been observed in recent experiments [15–18]. Such resonances between Bloch oscillations and the THz field have been the subject of intense experimental and theoretical investigations. An interesting open question concerns the influence of the radiation field on the quantum transport in semiconductor SLs. It is assumed that an ac field affects current anomalies due to resonances stemming from the quantizing dc electric and magnetic fields as well as polar-optical phonons. More importantly, one might expect additional peaks to emerge at the positions $l\Omega_{dc}+n\omega_c+m\omega\pm\omega_0=0$ (where ω_c is the cyclotron frequency, and l, n, and m are integers) when the SL is exposed to an intense radiation field of THz frequency. These cyclotron–Stark–phonon–photon (CSPP) resonances group round the cyclotron energy or the energy of polar-optical phonons well beyond the field regime, where resonances between Bloch oscillations and the radiation field appear (at $\Omega_{dc}=k\omega$). It is the main objective of our paper to investigate these new quantum effects in the SL transport.

Most theoretical studies of the SL miniband transport under THz irradiation were essentially one-dimensional in nature and based on the relaxation-time approximation, in which the equilibrium distribution function was introduced [19–26]. This approach as well as calculations using balance equations [27–29] cannot take into account quantum effects associated with the WS localization and the related current anomalies. This refers also to calculations [30, 31] using the model of sequential tunnelling together with the Tien–Gordon [32] or Tucker [33] expression for the ac current density. In the literature, there have appeared only few studies [34] of quantum effects in the SL transport under a radiation field.

We will treat the carrier transport in a SL under the influence of parallel electric and magnetic fields applied perpendicular to the SL layers in the WS and Landau quantized regime. The magnetic field enhances electro-phonon resonances appreciably and leads to additional magnetic-field-induced resonances. The current density is calculated within a microscopic quantum-kinetic approach that takes into account the heating of the lateral electron motion. Intra-collisional field effects (ICFEs) of all fields involved are considered. This allows a systematic study of CSPP resonances and the influence of the THz field on current anomalies.

2. The equation for the current density

A description of the field-mediated localization of carrier states requires an exact treatment of the external electric and magnetic fields. Considering the symmetry properties of correlation functions within the Wigner representation, a quantum-kinetic equation for the electron distribution function has been derived in the literature [35] for spatially homogeneous systems under the influence of electric and magnetic fields. This approach has been extended to account for an additional radiation field [34]. When the carrier density is small and electrons travel essentially only in the lowest miniband under the influence of electric and magnetic fields applied parallel to the SL axis, the time-dependent distribution function $f(\boldsymbol{k}|t)$ is calculated from [14]

$$\frac{\partial f(\boldsymbol{k}|t)}{\partial t}+\frac{eE_z(t)}{\hbar}\frac{\partial f(\boldsymbol{k}|t)}{\partial k_z}=\sum_{\boldsymbol{k}'}\int_{t_0}^{t}\mathrm{d}t'\ f(\boldsymbol{k}'|t')W(\boldsymbol{k}',\boldsymbol{k}|t',t) \qquad (1)$$

where

$$E_z(t)=E_{dc}+E_{ac}\cos\omega t$$

is the total time-dependent electric field. The Wigner-transformed scattering probability $W(\boldsymbol{k}',\boldsymbol{k}|t',t)$ comprises scattering-in and scattering-out contributions [35] arising, e.g., from the emission or absorption of polar-optical phonons [1] within the SL:

$$W(\boldsymbol{k}', \boldsymbol{k}|t', t) = \frac{4}{\hbar^2} \sum_{\boldsymbol{q},\lambda} |M_{q\lambda}|^2 |g(q_z)|^2 \,\mathrm{Re}\left[(N_{q\lambda}+1)\mathrm{e}^{-\mathrm{i}\omega_{q\lambda}(t-t')} + N_{q\lambda}\mathrm{e}^{\mathrm{i}\omega_{q\lambda}(t-t')}\right] \times \left\{ P\left(\boldsymbol{k}' + \frac{\boldsymbol{q}}{2}, \boldsymbol{k} - \frac{\boldsymbol{q}}{2}, \boldsymbol{q}\middle| t', t\right) - P\left(\boldsymbol{k}' + \frac{\boldsymbol{q}}{2}, \boldsymbol{k} + \frac{\boldsymbol{q}}{2}, \boldsymbol{q}\middle| t', t\right)\right\}. \tag{2}$$

$M_{q\lambda}$ is the electron–phonon coupling constant for phonons of wave vector $\boldsymbol{q}$ in branch λ. $g(q_z)$ is the form factor of the SL miniband calculated in the extreme tight-binding limit [36]. We use the simple bulk-phonon model because we think that besides the zone-folding effect most details of the electron–phonon interaction in a SL are not of great relevance for the high-field transport. In equation (2), $N_{q\lambda}$ denotes the equilibrium phonon distribution function and $\omega_{q\lambda}$ the phonon frequency. The ICFEs of all fields are included in the time-dependent Green's function [14] (see also reference [35, 37]):

$$P(\boldsymbol{k}', \boldsymbol{k}, \boldsymbol{q}|t', t) = \exp\left\{ -\frac{\mathrm{i}}{\hbar} \int_0^{t-t'} \mathrm{d}t'' \left[\varepsilon\left(\boldsymbol{k}' + \frac{\boldsymbol{q}}{2} + \frac{e}{\hbar}\int_{t'}^{t'+t''} \mathrm{d}\tau\, \boldsymbol{E}(\tau) + \boldsymbol{A}(\mathrm{i}\boldsymbol{\nabla}_{k'})\right) - \varepsilon\left(\boldsymbol{k}' - \frac{\boldsymbol{q}}{2} + \frac{e}{\hbar}\int_{t'}^{t'+t''} \mathrm{d}\tau\, \boldsymbol{E}(\tau) - \boldsymbol{A}(\mathrm{i}\boldsymbol{\nabla}_{k'})\right)\right]\right\} \delta_{\boldsymbol{k}', \boldsymbol{k} + (e/\hbar)\int_t^{t'} \mathrm{d}\tau\, \boldsymbol{E}(\tau)} \tag{3}$$

which expresses the fact that in strong electric fields neither the quasi-momentum $\boldsymbol{k}$ nor the energy are conserved. $\boldsymbol{A}(\boldsymbol{k})$ is the vector potential of the magnetic field in the symmetric gauge. The band structure $\varepsilon(\boldsymbol{k}) = \hbar^2\boldsymbol{k}_\perp^2/2m^* + \Delta(1 - \cos k_z d)/2$ of the lowest miniband is non-parabolic along the SL axis and describes electrons moving freely with the transverse quasi-momentum $\hbar\boldsymbol{k}_\perp$ and the effective mass m^* within the SL wells. Δ is the miniband width. A kinetic equation of the form (1) to (3) has also been derived using non-equilibrium Green functions in [38]. The authors of that paper obtained a similar result with the essential difference that in their approach the quasi-momentum conservation remained incorrectly intact.

In our derivation of a final kinetic equation we will progressively employ the discrete nature of the underlying energy spectrum. For a sinusoidal ac electric field with a frequency ω, the distribution function is periodic in time ($f(\boldsymbol{k}|t + 2\pi/\omega) = f(\boldsymbol{k}|t)$). It is, therefore, convenient to perform a Fourier transformation

$$f(\boldsymbol{k}|t) = \sum_{m=-\infty}^{\infty} \mathrm{e}^{\mathrm{i}m\omega t} f_m(\boldsymbol{k}). \tag{4}$$

According to equation (1) the Fourier coefficients $f_m(\boldsymbol{k})$ obey the equation

$$\mathrm{i}m\omega f_m(\boldsymbol{k}) + \frac{eE_{dc}}{\hbar}\frac{\partial f_m(\boldsymbol{k})}{\partial k_z} + \frac{eE_{ac}}{2\hbar}\left(\frac{\partial f_{m+1}(\boldsymbol{k})}{\partial k_z} + \frac{\partial f_{m-1}(\boldsymbol{k})}{\partial k_z}\right) = \sum_{\boldsymbol{k}'}\sum_{m'} f_{m'}(\boldsymbol{k}') W_{m'm}(\boldsymbol{k}', \boldsymbol{k}) \tag{5}$$

where the field-dependent matrix elements of the collision integral are given by

$$W_{m'm}(\boldsymbol{k}', \boldsymbol{k}) = \frac{\omega}{2\pi}\int_0^{2\pi/\omega} \mathrm{d}t\, \mathrm{e}^{\mathrm{i}(m'-m)\omega t} \int_0^\infty \mathrm{d}t'\, \mathrm{e}^{-\mathrm{i}m'\omega t'} W(\boldsymbol{k}', \boldsymbol{k}, t - t', t). \tag{6}$$

In the derivation of equation (6), we assumed that the external fields had been switched on at a time $t_0 \to -\infty$. For the alignment of the electric and magnetic fields considered, parallel to the SL axis, the lateral electron motion is spherically symmetric, i.e. , $f_m(\boldsymbol{k}) = f_m(|\boldsymbol{k}_\perp|, k_z)$. We will conveniently employ also another symmetry property of the system, namely the periodicity of the distribution function [1] along the field direction ($f_m(k_\perp, k_z+2\pi/d) = f_m(k_\perp, k_z)$). All of these symmetries are accounted for in the following *ansatz* for the distribution function [4]:

$$f_m(\boldsymbol{k}) = 2\pi l_B^2 n_s \mathrm{e}^{-k_\perp^2 l_B^2} \sum_{n=0}^{\infty} (-1)^n L_n(2k_\perp^2 l_B^2) \sum_{l=-\infty}^{\infty} \mathrm{e}^{\mathrm{i}lk_z d} f_{mn}^l \tag{7}$$

where l_B is the magnetic length, n_s the electron sheet density, and L_n are Laguerre polynomials. As a consequence of charge conservation, the unknown numbers f_{mn}^l satisfy the normalization condition

$$\sum_{n=0}^{\infty} f_{0n}^0 = 1 \tag{8}$$

which guarantees that the homogeneous set of kinetic equations (5) has a unique non-trivial solution. To elucidate the main physical aspects characterizing CSPP resonances in the SL transport, the details of the screened electron–phonon coupling matrix elements are probably not of great relevance. Therefore, we will avoid complications arising from the momentum integrals in equation (2) by considering constant matrix elements and dispersionless optical phonons:

$$|M_{\boldsymbol{q}\lambda}|^2 |g(q_z)|^2 \to \omega_0^2 \Gamma. \tag{9}$$

Here Γ is the coupling constant. Inserting the *ansatz* (7) into equation (5) and calculating the integrals over the transverse momenta [4, 14], we obtain

$$\begin{aligned}
(\mathrm{i}m\omega + \mathrm{i}l\Omega_{dc}) f_{mn}^l &+ \frac{\mathrm{i}}{2} l\Omega_{ac}(f_{m-1n}^l + f_{m+1n}^l) = P_{mn}^l \\
&= \frac{2\omega_0^2\Gamma}{\pi\hbar^2 l_B^2 d} \sum_{n'=0}^{\infty} \sum_{l',m'=-\infty}^{\infty} \left(\frac{d}{2\pi}\right)^2 \int_0^{2\pi/d} \mathrm{d}k_z\, \mathrm{d}k_z'\, \mathrm{e}^{\mathrm{i}(l'k_z' - lk_z)d} \\
&\times \frac{\omega}{2\pi} \int_0^{2\pi/\omega} \mathrm{d}t\, \mathrm{e}^{\mathrm{i}(m'-m)\omega t} \int_0^{\infty} \mathrm{d}t'\, \mathrm{e}^{-st' - \mathrm{i}m'\omega t'} \\
&\times \left\{ f_{m'n'}^{l'} \,\mathrm{Re}\left[\Phi(t')\mathrm{e}^{\mathrm{i}\omega_c t'(n'-n)} P_{z-}(k_z', k_z|t-t', t)\right] \right. \\
&\left. - f_{m'n}^{l'} \,\mathrm{Re}\left[\Phi(t')\mathrm{e}^{\mathrm{i}\omega_c t'(n-n')} P_{z+}(k_z', k_z|t-t', t)\right] \right\}
\end{aligned} \tag{10}$$

with the abbreviation

$$\Phi(t) = (N_0 + 1)\mathrm{e}^{-\mathrm{i}\omega_0 t} + N_0 \mathrm{e}^{\mathrm{i}\omega_0 t}. \tag{11}$$

$\Omega_{ac} = eE_{ac}d/\hbar$ is the Bloch frequency of the ac field. A finite lifetime of the discrete energy states is accounted for in equation (10) by a phenomenological parameter s. In deriving equation (10) we profited from the fact that the Green function P in equation (3) factorizes with respect to the $\boldsymbol{k}_\perp$- and k_z-dependencies. Effects exerted by the electric fields during the scattering process are described by the function

$$P_{z\pm}(k_z', k_z|t', t) = \sum_{q_z} P_z\left(k_z' + \frac{q_z}{2}, k_z \pm \frac{q_z}{2}, q_z \middle| t', t\right) \tag{12}$$

which depends on two time arguments. The remaining k_z-, k_z'-integrals in equation (10) are easily calculated using equation (3) and recalling the identity

$$\begin{aligned}
\frac{1}{2\pi}\int_0^{2\pi} \mathrm{d}x\, &\exp\left[-\mathrm{i}(lx + a\sin x + b\cos x)\right] \\
&= \mathrm{e}^{\mathrm{i}l\varphi_z} J_l(\sqrt{a^2+b^2}) \times \begin{cases} (-1)^l & \text{if } a \geqslant 0 \\ 1 & \text{otherwise} \end{cases}
\end{aligned} \tag{13}$$

with

$$\varphi_z = \arctan(b/a). \tag{14}$$

The scattering term P^l_{mn} entering the kinetic equation (10) now simplifies considerably and takes the form

$$P^l_{mn} = \frac{4\omega_0^2\Gamma}{\pi\hbar^2 l_B^2 d} \sum_{n'=0}^{\infty} f^0_{0n'} \int_0^{\infty} dt'\ e^{-st'}\ \mathrm{Im}\left[\Phi(t')e^{i\omega_c t'(n'-n)}\right] F^l_m(t') \tag{15}$$

where we used the definitions

$$F^l_m(t') = \frac{\omega}{2\pi}\int_0^{2\pi/\omega} dt\ \exp\left(-im\omega t - il\frac{\Omega_{ac}}{\omega}\sin\omega t\right)P^l(t,t') \tag{16}$$

and

$$P^l(t,t') = e^{il\varphi_z(t,t')}\frac{1}{\pi}\int_0^{\pi} dy\ \sin y J_l\left(\frac{\Delta}{\hbar}\sin y|Z(t,t')|\right)\times\begin{cases}(-1)^l & \text{if } \mathrm{Re}\, Z \geqslant 0\\ 1 & \text{otherwise.}\end{cases} \tag{17}$$

In equation (17), J_l is the Bessel function and the complex function $Z(t,t')$ is expressed by a time integral

$$\begin{aligned} Z(t,t') = |Z|e^{i\varphi_z} &= \int_0^{t'} dt''\ \exp\left[-i\left(\Omega_{dc}t'' - \frac{\Omega_{ac}}{\omega}\sin\omega(t-t'')\right)\right] \\ &= i\sum_{k=-\infty}^{\infty}\frac{J_k(\Omega_{ac}/\omega)}{\Omega_{dc}+k\omega}e^{ik\omega t}\left[e^{-i(\Omega_{dc}+k\omega)t'} - 1\right] \end{aligned} \tag{18}$$

which has been calculated by considering equations (27) and (30) in the appendix. In equation (10) only the t'-integral leads to poles associated with CSPP resonances. From equations (10) and (18), it is seen that CSPP resonances are expected to occur at the positions $l\Omega_{dc} + n\omega_c + m\omega \pm \omega_0 = 0$, with l, m, and n being integers.

Throughout, we refer to a dc electric field strength, at which WS localization prevails ($\Omega_{dc}\tau > 1$). In this case, a perturbational treatment of scattering has become a suitable tool [1] for determining the high-field transport properties. Under the condition $\Omega_{dc}\tau > 1$, it is sufficient to retain only the time-averaged zeroth Fourier components of the distribution function in the scattering integral, which implies replacing the numbers $f^{l'}_{m'n'}$ by $\delta_{l',0}\delta_{m',0}f^0_{0n'}$ there. As shown in the appendix, the resulting kinetic equation can be solved exactly. The solution has the form

$$f^l_{0n} = \sum_{m=-\infty}^{\infty}\frac{P^l_{mn}}{il\Omega_{dc}}S^l_m \tag{19}$$

with

$$S^l_m = \sum_{k=-\infty}^{\infty} J_{k-m}\left(l\frac{\Omega_{ac}}{\omega}\right)J_k\left(l\frac{\Omega_{ac}}{\omega}\right)\frac{il\Omega_{dc}+1/\tau_{ac}}{i(l\Omega_{dc}+k\omega)+1/\tau_{ac}}. \tag{20}$$

In equation (20), we introduced a phenomenological scattering time τ_{ac}, which prevents the distribution function from diverging at the resonance positions $\Omega_{dc} = k\omega$. If there were no ac electric field ($\Omega_{ac} \to 0$), we would have from equation (20) $S^l_m = \delta_{m,0}$. The solution (19) of equation (10) fulfils the important requirement that in the limit $\Omega_{ac} \to 0$ (but $\Omega_{dc} \neq 0$) the non-equilibrium distribution function $(f^l_n)_{dc} = P^l_{0n}/il\Omega_{dc}$ for a biased electron system is recovered and not the equilibrium distribution as in all former theoretical approaches [19–26]. Once the distribution function has been determined from the kinetic equation, it is straightforward to calculate the current density from

$$j_z(t) = \frac{e}{\hbar V} \sum_{\boldsymbol{k}} \frac{\partial \varepsilon(\boldsymbol{k})}{\partial k_z} f(\boldsymbol{k}|t). \tag{21}$$

Inserting the tight-binding dispersion relation as well as equations (4) and (7) into this equation, we arrive at

$$j_z = \frac{en_s\Delta}{4\hbar} \frac{1}{2\mathrm{i}} \sum_{n=0}^{\infty} (f_{0n}^{-1} - f_{0n}^{1}). \tag{22}$$

For the simple cosine energy band only the $l = \pm 1$ elements of the distribution function f_{0n}^l enter the expression for the current density. To proceed further in calculating the current, the formal solution (19) is inserted into equation (22). From equation (15) it is seen that the matrix element P_{mn}^l itself depends on the components f_{0n}^0 of the lateral distribution function. For simplicity we will not go into a detailed analysis of the lateral carrier heating within the wells but will make use of the Boltzmann distribution function [4]

$$f_{0n}^0 = 2\sinh\left(\frac{\hbar\omega_c}{2k_BT}\right) \exp\left[-\frac{\hbar\omega_c}{k_BT}(n + 1/2)\right] \tag{23}$$

which allows us to calculate the n'-sum in equation (15) analytically. For the current density we obtain the following final expression:

$$j_z = \frac{en_s\Delta}{\hbar\Omega_{dc}} \frac{m^*\omega_0\omega_c\Gamma}{\pi\hbar^3 d} \frac{1 - \exp(-\hbar\omega_c/k_BT)}{1 - \exp(-\hbar\omega_0/k_BT)} \sum_{n=0}^{\infty} \sum_{m=-\infty}^{\infty} \left[\mathrm{Re}\, Q_{mn}^1 \,\mathrm{Re}\, S_m^1 - \mathrm{Im}\, Q_{mn}^1 \,\mathrm{Im}\, S_m^1\right] \tag{24}$$

with

$$Q_{mn}^1 = \int_0^{\infty} \mathrm{d}t'\, \mathrm{e}^{-st'}\, \mathrm{Im}\left[\frac{\mathrm{e}^{-\mathrm{i}n\omega_c t'}(\mathrm{e}^{-\mathrm{i}\omega_0 t'} + \mathrm{e}^{-\hbar\omega_0/k_BT}\mathrm{e}^{\mathrm{i}\omega_0 t'})}{1 - \mathrm{e}^{-\hbar\omega_c/k_BT}\mathrm{e}^{\mathrm{i}\omega_c t'}}\right] F_m^1(t'). \tag{25}$$

The current density (24) is composed of two different contributions, which correspond to the two transport channels opened up by carrier scattering or delocalization induced by the radiation field. When the ac electric field vanishes ($\Omega_{ac} = 0$), only the first current contribution remains on the right-hand side of equation (24). This term describes scattering-mediated carrier transport in the presence of a strong dc electric field, characterized by the antisymmetric part ($\sim \mathrm{Re}\, Q_{0n}^1$) of the non-equilibrium distribution function. A radiation field gives rise to an additional current contribution (the second term on the right-hand side of equation (24)), which results from photon-mediated delocalization of carriers. This term, which is negative, describes the effect whereby Bloch-oscillating carriers absorb energy from the radiation field to travel against the field direction [14]. If this current component is small compared to the scattering-induced part, it is sufficient to retain only the $m = 0$ term [29] in the m-sum of equation (24).

3. Numerical results and discussion

Negative current and Bloch–photon resonances at $\Omega_{dc} = k\omega$ have been observed at a comparatively small dc bias [15]. However, at low dc electric fields, our approach is not applicable, as we used only the lateral component of the distribution function in the collision integral, which results in an asymptotic $1/E_{dc}$ dependence of the current. We will focus on high electric and magnetic field strengths, where pronounced resonance structures are predicted to appear in the current density unless they are smeared out by collisional broadening. For the parameters used in our numerical calculation, the results are dominated by the $m = 0$ term in equation (24).

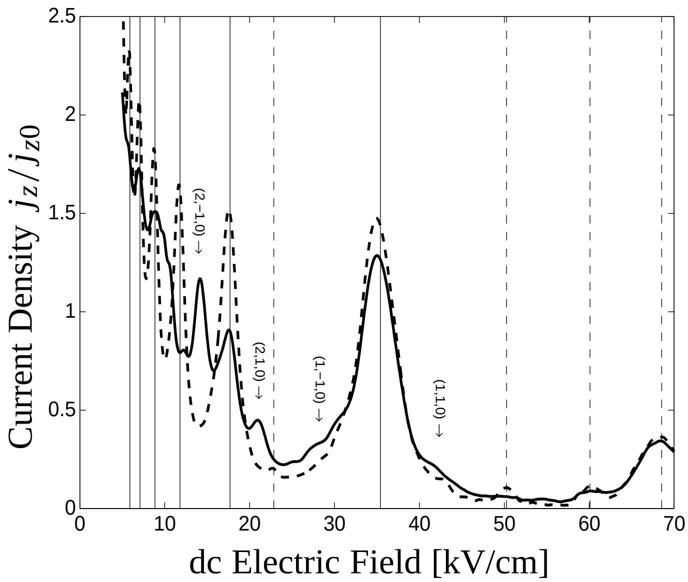

Figure 1. The electric field dependence of the current density measured in units of $j_{z0} = en_s\Delta m^*\omega_0\Gamma/\pi\hbar^4 d$ for $\Omega_{ac}/\omega = 0$ (dashed curve) and $\Omega_{ac}/\omega = 0.5$ (solid curve). We used the following parameters: $\Delta/\hbar\omega_0 = 1$, $\hbar\omega_0/k_B T = 5$, $\omega/\omega_0 = 0.2$, and $H = 20$ T, and introduced two phenomenological broadening parameters $1/\omega_0\tau_{dc} = 0.07$, $1/\omega_0\tau_{ac} = 0.05$, where $\tau_{dc} = 1/s$ is the relaxation time of the dc transport. The SL period is $d = 10$ nm. Vertical solid and dashed lines mark the positions of cyclotron–Stark–phonon resonances. CSPP resonances are denoted by arrows.

Numerical results for the electric field dependence of the current density are shown in figure 1 for $\Omega_{ac}/\omega = 0$ (dashed curve) and $\Omega_{ac}/\omega = 0.5$ (solid curve). If there were no THz field (dashed curve), pronounced electro-phonon resonances would appear, which are marked by vertical solid lines. These resonances are strongly enhanced by a magnetic field (for figure 1 we used $H = 20$ T). In addition, minor peaks are observed at cyclotron–Stark–phonon resonance positions, marked by vertical dashed lines. As illustrated by the solid curve, a THz radiation field rounds off these sharp resonance structures. To what extent the radiation field is effective in smoothing current peaks depends on the value of the dc bias. An intense THz field leads also to the appearance of additional current maxima at CSPP resonance positions, marked by arrows and numbers (l, m, n) (in figure 1), for which the resonance condition $l\Omega_{dc} = m\omega + n\omega_c + \omega_0$ is fulfilled. The proportion of new current anomalies that arise depends sensitively on the dc electric field. CSPP resonances can easily be discriminated from Bloch–photon-type resonances at $\Omega_{dc} = k\omega$, because in the former the frequency ω_0 of polar-optical phonons is involved. The above-mentioned peculiarities in the I–V characteristic result from ICFEs of the ac field. For the parameters used in our calculation, the ac-field-induced current component, described by the second term on the right-hand side of equation (24), is negligibly small.

A second example is shown in figure 2, where the dashed curve is again the reference curve for $\Omega_{ac}/\omega = 0$, but this time for a smaller miniband width ($\Delta/\hbar\omega_0 = 0.5$). In addition,

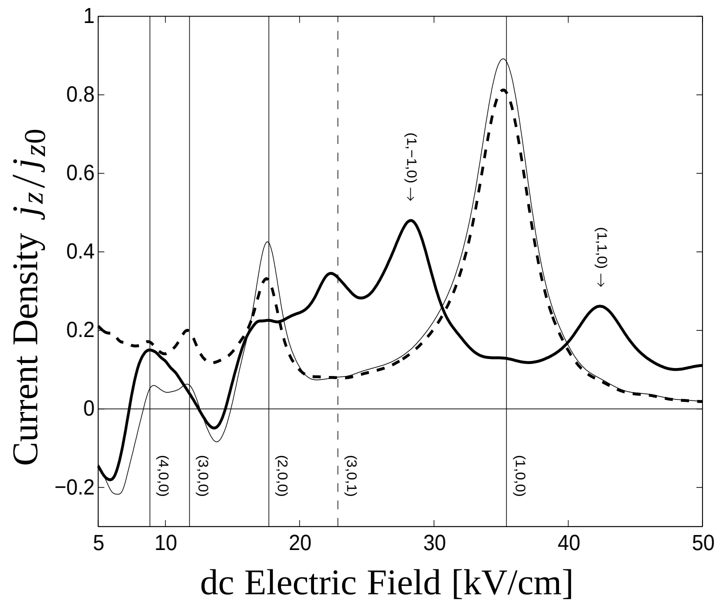

Figure 2. As figure 1, but for $\Omega_{ac}/\omega = 0$ (dashed curve) and $\Omega_{ac}/\omega = 2$ (thick solid curve). In addition, we used $\Delta/\hbar\omega_0 = 0.5$. The thin solid curve has been calculated by neglecting the ICFEs of the THz field.

the intensity of the THz field is larger ($\Omega_{ac}/\omega = 2$ for the thick solid curve). The application of such an intense laser field leads to a negative current density and to an almost complete disappearance of electro-phonon resonances marked by vertical solid lines. New maxima appear at CSPP resonance positions indicated by arrows and the numbers (l, m, n). Under the participation of the photon field, the cyclotron–Stark–phonon resonance marked by the vertical dashed line is considerably enhanced. All of these new pronounced structures in the I–V characteristic are due to ICFEs. This is shown by the thin solid curve, which has been calculated without taking into account the influence of the ac field on scattering [14]. The classical treatment of the THz field reproduces the I–V dependence at comparatively low electric fields, where the current becomes negative, but does not account for the appearance of pronounced CSPP resonances, which are due to quantum-mechanical effects.

The magnetic field dependence of the current density is depicted in figure 3 for $\Omega_{ac}/\omega = 0$ (dashed curve) and $\Omega_{ac}/\omega = 1$ (solid curve). The positions of cyclotron–Stark–phonon resonances are shown by vertical solid ($l = 0$), dashed ($l = 1$), and dash–dotted ($l = 2$) lines. For the set of parameters used in this calculation, a number of weak CSPP resonances emerge in the current density, marked by arrows and numbers (l, m, n), which fulfil the resonance condition $n\omega_c = l\Omega_{dc} + m\omega + \omega_0$. An observation of these new resonances would require SL samples for which the collisional broadening is extremely small. Pronounced resonance peaks in the current density, which occur when $\Omega_{ac} = 0$ (dashed curve), become considerably smoother when an intense ac field is applied to the SL. It is seen from figure 1 that whether the current is reduced or enhanced by switching on the ac field depends on the dc electric field strength. For the dc electric field that we used in figure 2 ($E_{dc} = 35.4$ kV cm^{-1} or $\Omega_{dc} = \omega_0$), the ac field leads to a current reduction, the extent of which increases with increasing magnetic field. At low intensities of the THz field, the predicted CSPP resonance peaks in the current density are less pronounced than the already-studied cyclotron–Stark–phonon resonances.

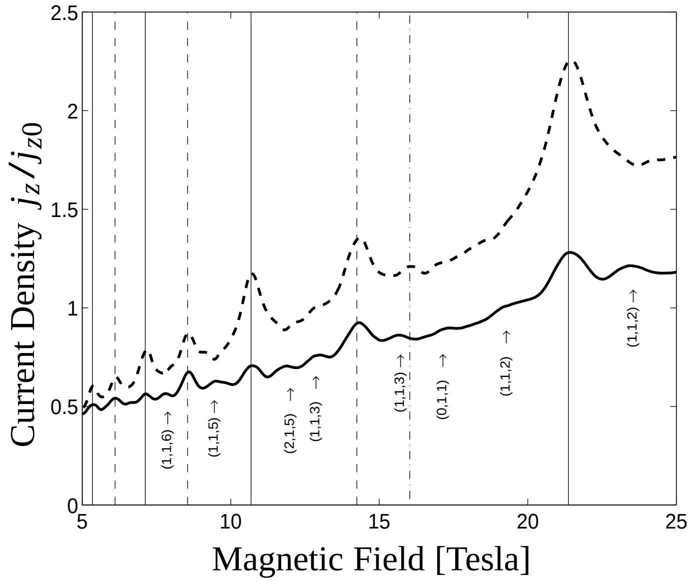

Figure 3. The magnetic field dependence of the current density measured in units of $j_{z0} = en_s \Delta m^* \omega_0 \Gamma / \pi \hbar^4 d$ for $\Omega_{ac}/\omega = 0$ (dashed curve) and $\Omega_{ac}/\omega = 1$ (solid curve). We used the set of parameters $\Delta/\hbar\omega_0 = 1$, $\hbar\omega_0/k_B T = 1$, $\omega/\omega_0 = 0.2$, and $E_{dc} = 35.4$ kV cm^{-1}. The broadening parameters are the same as in figure 1. Vertical lines mark the positions of cyclotron–Stark–phonon resonances. CSPP resonances are denoted by arrows.

The collisional broadening plays an exceptional role in the system considered in which the energy spectrum is discrete due to WS and Landau quantization. Without any lifetime broadening, the I–V characteristics are given by a set of δ-functions located at numerous resonance positions. In our approach a smooth I–V characteristic is obtained by introducing phenomenological broadening parameters related to the dc- and ac-field effects. Depending on the values of these parameters, the predicted new quantum-mechanical resonances can appear or be completely smeared out. This is a serious disadvantage of our calculation. Reliable quantitative results can only be derived when both ICFEs and collisional broadening are accounted for within the same microscopic quantum-mechanical approach. Further progress will be related to studying quantum transport in SLs within this framework.

4. Summary

We treated the influence of a strong THz radiation field on the quantum transport of carriers in the lowest miniband of a SL subject to quantizing dc electric and magnetic fields. All external fields are applied parallel to the SL axis. ICFEs of all fields as well as the heating of the lateral carrier motion are taken into account within a quantum-kinetic approach. The radiation field gives rise to new CSPP resonances occurring when the four frequencies Ω_{dc}, ω_c, ω, and ω_0 fulfil the resonance condition $l\Omega_{dc} + n\omega_c + m\omega \pm \omega_0 = 0$ (where l, n, m are integers). Depending on the intensity of the THz field, even pronounced structures are predicted to appear at these resonance positions both in the electric and magnetic field dependences of the current density.

To our knowledge, electro-phonon resonances have not been reported in SL transport experiments until now. Nevertheless, enhanced LO-phonon-assisted inter-Landau-level tunnel peaks have been observed in recent experiments on a GaAs/AlGaAs triple-barrier tunnel diode [39]. It was also possible to study elastic cyclotron–Stark transport anomalies for rather different SLs [6, 10]. An observation of the predicted new quantum-mechanical CSPP transport resonances requires SLs in which collisional broadening is extremely small. A further prediction of our approach is that existing strong current maxima at cyclotron–Stark–phonon resonance positions should be strongly suppressed by an intense THz field.

Appendix

In this appendix we will derive the exact formal solution of the kinetic equation (10). To that end, equation (4) is used to reintroduce the time-dependent distribution function $f_n^l(t)$, which, according to equation (10), satisfies the first-order differential equation

$$\frac{\mathrm{d}f_n^l(t)}{\mathrm{d}t} + \mathrm{i}\frac{\mathrm{d}A_l(t)}{\mathrm{d}t} f_n^l(t) = P_n^l(t) \tag{A.1}$$

with

$$A_l(t) = l\Omega_{dc}t + A_{ac}(t) \qquad A_{ac}(t) = l\frac{\Omega_{ac}}{\omega}\sin\omega t. \tag{A.2}$$

Equation (26) is easily solved. We obtain

$$f_m^l(t) = \mathrm{e}^{-\mathrm{i}A_l(t)}\left[C + \int_0^t \mathrm{d}t'\ P_n^l(t')\mathrm{e}^{\mathrm{i}A_l(t')}\right] \tag{A.3}$$

where the periodicity condition $f_n^l(t + 2\pi/\omega) = f_n^l(t)$ is used to determine the integration constant C:

$$C = \int_{-2\pi/\omega}^0 \mathrm{d}\tau\ P_n^l(\tau)\mathrm{e}^{\mathrm{i}A_l(\tau)}/(1 - \mathrm{e}^{-2\pi\mathrm{i}l\Omega_{dc}/\omega}). \tag{A.4}$$

The remaining integrals over time variables are calculated using

$$\mathrm{e}^{\mathrm{i}A_{ac}(t)} = \sum_{k=-\infty}^{\infty} J_k\left(l\frac{\Omega_{ac}}{\omega}\right)\mathrm{e}^{\mathrm{i}k\omega t}. \tag{A.5}$$

The final result is

$$f_n^l(t) = \mathrm{e}^{-\mathrm{i}A_l(t)}\sum_{k,m=-\infty}^{\infty} P_{mn}^l J_k\left(l\frac{\Omega_{ac}}{\omega}\right)\frac{\mathrm{e}^{\mathrm{i}(l\Omega_{dc}+(k+m)\omega)t}}{\mathrm{i}(l\Omega_{dc} + (k+m)\omega)}. \tag{A.6}$$

Applying equation (30) again, we obtain

$$f_{0n}^l = \sum_{k,m=-\infty}^{\infty} P_{mn}^l \frac{J_{k-m}(l\Omega_{ac}/\omega)J_k(l\Omega_{ac}/\omega)}{\mathrm{i}(l\Omega_{dc} + k\omega)} \tag{A.7}$$

for the time-averaged components of the distribution function. To avoid divergencies appearing on the right-hand side of equation (32) at $l\Omega_{dc} + k\omega = 0$, we introduce a phenomenological scattering time τ_{ac} and arrive at equations (19) and (20).

Acknowledgment

The authors acknowledge financial support by the Deutsches Zentrum für Luft- und Raumfahrt.

References

[1] Bryksin V V and Firsov Y A 1971 *Zh. Eksp. Teor. Fiz.* **61** 2373 (Engl. Transl. 1971 *Sov. Phys.–JETP* **34** 1272)
[2] Bryksin V V and Kleinert P 1997 *J. Phys. C: Solid State Phys.* **9** 7403
[3] Rott S, Binder P, Linder N and Döhler G H 1998 *Physica* E **2** 511
[4] Kleinert P and Bryksin V V 1997 *Phys. Rev.* B **56** 15 827
[5] Noguchi H, Sakaki H, Takamasu T and Miura N 1992 *Phys. Rev.* B **45** 12 148
[6] Canali L, Lazzarino M, Sorba L and Beltram F 1996 *Phys. Rev. Lett.* **76** 3618
[7] Claro F, Weisz J F, Müller W, von Klitzing K, Grahn H T and Ploog K 1996 *Phys. Rev.* B **53** 7970
[8] Canali L, Beltram F, Lazzarino M and Sorba L 1997 *Superlatt. Microstruct.* **22** 155
[9] Nogaret A, Eaves L, Main P C, Henini M, Maude D K and Portal J C 1997 *Phys. Status Solidi* b **204** 374
[10] Liu J, Gornik E, Xu S and Zheng H 1997 *Semicond. Sci. Technol.* **12** 1422
[11] Polyanovskii V M 1981 *Fiz. Tekh. Poluprov.* **15** 2051 (Engl. Transl. 1981 *Sov. Phys.–Semicond.* **15** 1190)
[12] Ferreira R 1991 *Phys. Rev.* B **43** 9336
[13] Shon N H and Nazareno H N 1997 *Phys. Rev.* B **55** 6712
[14] Bryksin V V and Kleinert P 1999 *Phys. Rev.* B at press
[15] Keay B J, Zeuner S, Allen J S J, Maranowski K D, Gossard A C, Bhattacharya U and Rodwell M J W 1995 *Phys. Rev. Lett.* **75** 4102
[16] Keay B J, Allen J S J, Galan J, Kaminski J P, Campman K L, Gossard A C, Bhattacharya U and Rodwell M J W 1995 *Phys. Rev. Lett.* **75** 4098
[17] Zeuner S, Keay B J, Allen J S J, Maranowski K D, Gossard A C, Bhattacharya U and Rodwell M J W 1996 *Phys. Rev.* B **53** R1717
[18] Unterrainer K, Keay B J, Wanke M C, Allen J S J, Leonard D, Medeiros-Ribeiro G, Bhattacharya U and Rodwell M J W 1996 *Phys. Rev. Lett.* **76** 2973
[19] Ignatov A A and Romanov Y A 1975 *Fiz. Tverd. Tela* **17** 3388 (Engl. Transl. 1976 *Sov. Phys.–Solid State* **17** 2216)
[20] Ignatov A A and Romanov Y A 1976 *Phys. Status Solidi* b **73** 327
[21] Pavlovich V V and Epshtein E M 1976 *Sov. Phys.–Semicond.* **10** 1196
[22] Mensah S Y 1992 *J. Phys.: Condens. Matter* **4** L325
[23] Yevtushenko O M 1996 *Phys. Rev.* B **54** 2578
[24] Nazareno H N and Masut R A 1997 *Solid State Commun.* **101** 819
[25] Zhao X G, Georgaki G A and Niu Q 1997 *Phys. Rev.* B **56** 3976
[26] Caetano E W S, Mendes E A, Freire V N, da Costa J A P and Lei X L 1998 *Phys. Rev.* B **57** 11 872
[27] Lei X L, Dong B and Chen Y Q 1997 *Phys. Rev.* B **56** 12 120
[28] Xia J B 1998 *Phys. Rev.* B **58** 3565
[29] Lei X L and Cui H L 1998 *Eur. Phys. J.* B **4** 513
[30] Platero G and Aguado R 1997 *Appl. Phys. Lett.* **70** 3546
[31] Wacker A, Jauho A P, Zeuner S and Allen S J 1997 *Phys. Rev.* B **56** 13 268
[32] Tien P K and Gordon J P 1963 *Phys. Rev.* B **129** 647
[33] Tucker J R 1979 *IEEE J. Quantum Electron.* **15** 1234
[34] Polyanovskii V M 1980 *Fiz. Tverd. Tela* **22** 1975 (Engl. Transl. 1980 *Sov. Phys.–Solid State* **22** 1151)
[35] Bryksin V V and Firsov Y A 1973 *Fiz. Tverd. Tela* **15** 3235 (Engl. Transl. 1973 *Sov. Phys.–Solid State* **15** 2158)
[36] Lei X L, Horing N J M and Cui H L 1992 *J. Phys.: Condens. Matter* **4** 9375
[37] Bryksin V V, Woloschin V C and Rajtzev A W 1980 *Fiz. Tverd. Tela* **22** 3076 (Engl. Transl. 1980 *Sov. Phys.–Solid State* **22** 1796)
[38] Khan F S, Davis J H and Wilkins J W 1987 *Phys. Rev.* B **36** 2578
[39] Wirner C, Awano Y, Mori T, Yokoyama N, Nakagawa T, Bando H and Muto S 1996 *Appl. Phys. Lett.* **69** 1596